Chapter

Experimental Study of Adsorption on Activated Carbon for CO_2 Capture

Hesham G. Ibrahim and Mohamed A. Al-Meshragi

Abstract

The adsorption of carbon dioxide (CO_2) on activated carbon (AC) prepared from olive trees has been investigated by using a fixed bed adsorption apparatus. The adsorption equilibrium and breakthrough curves were determined at different temperatures 30, 50, 70, and 90°C in order to investigate both kinetic and thermodynamic parameters. Maximum CO_2 sorption capacity on AC ranged from 109.5 to 35.46 and from 129.65 to 35.55 mg CO_2/g of AC for initial concentrations 10 and 13.725% vol., respectively. Different isotherm models are applied to mathematically model the CO_2 adsorption, and on the basis of the estimated adsorption capacity by model and determination coefficient (r^2), the Langmuir model provides a perfect fit to the experimental data owing to closeness of the r^2 to unity. From the correlation coefficient, it is found that the pseudo-second-order model is well-fitted with the experimental data. In addition, it indicates that CO_2 adsorption is a physical adsorption process and demonstrates a behavior of an exothermic reaction, which is consistent with the thermodynamic analysis. The results obtained in this study conclude that AC prepared from olive trees can be considered as adequate for designing a fixed bed cycle to separate carbon dioxide from flue gases and serve as a benchmark while searching for inexpensive and superior activated carbon production in future studies.

Keywords: adsorption, breakthrough, equilibrium, kinetic, thermodynamic

1. Introduction

The emissions of CO_2 from burn fossil fuels are the major reason for the increase in the concentration of this gas in the atmosphere [1]. The amount of carbon dioxide in the atmosphere is currently increasing globally by around 6 billion tons per year [2].

A feasible technique method used industrially in reduction of CO_2 emissions is capture and storage. CO_2 capture means separating the CO_2 from other gases in flue. The advanced technologies being used worldwide for CO_2 capture in different arrangements are post-combustion, pre-combustion, and oxy-fuel processes [1].

Numerous investigations have been done for CO_2 capture field by using adsorption, which are indicating to the effective usage of a post-combustion treatment of gas emissions of flue. The proposed schemes in a cycle process of capture by adsorption include pressure swing adsorption (PSA) and temperature swing

adsorption (TSA) [1, 3–5]. The capture of carbon dioxide by adsorptive process is mainly based on preferential adsorption of this gas on a porous adsorbent. Thus, the first and most important step is to find a suitable adsorbent [1]. Carbon materials are relatively insensitive to moisture and are suitable candidates for CO_2 capture due to their pore structure and surface chemistry properties [6].

In recent years, considerable attention has been focused on removal of pollutants by using adsorbents derived from low-cost agro-wastes. Olive trees (*Olea europaea*) are abundantly found and easily available in the Mediterranean countries generally and especially Libya. Thus, the aim of the present study is to describe the dynamics and equilibrium of CO_2-N_2 mixture adsorption on local activated carbon (AC) prepared from olive trees using the breakthrough curve method. Experimental breakthrough curves are used to obtain equilibrium data, and then Langmuir, Freundlich, Temkin, and Dubinin-Radushkevich equilibrium adsorption models were applied. Kinetic models examined herein are simple first-order, pseudo-first-order, pseudo-second-order, and intra-particle diffusion. Model validity with experimental data is assessed by using the coefficient of determination (r^2); the closer the value to unity means that the model will be better. Thermodynamic analysis of adsorption of CO_2 on AC estimates the values of enthalpy, free energy, and entropy. Also, effects of the interaction between CO_2 and NO are studied.

2. Materials and methods

2.1 Preparation of activated carbon

The prepared activated carbon based on charcoal was prepared from olive trees for low cost and was abundantly available. The used activated carbon was obtained from the local area. The raw material of charcoal as received was crushed, ground, and sieved, and only the fraction of particle size 5 mm was chosen as the mean particle diameter. Then it is heated in an oven for 48 h up to 115°C to dry and activate (to remove the absorbed gases and moisture it contains) [7, 8]. The produced activated carbon is then stored in a tightly closed container to be used as required. The total pore volume and surface area of AC were determined using Gemini VII 2390a analyzer. The particle size is obtained by using standard mesh sieves (standard sieve AS 200), and average value of bed porosity is calculated in terms of the average diameter of particles [9].

2.2 Dynamic adsorption capacity of carbon dioxide

A laboratory system used for measuring breakthrough curve was set up and shown in **Figure 1**. The adsorber which is made of carbon steel tube, consists of three zones:

- Calming zone with 6.5 cm diameter and 8 cm length containing spherical particles of carbon steel.
- Active zone with 8.44 cm diameter and 39 cm length containing the activated carbon particles, and it was surrounded by a shell containing a heating medium.
- Ending zone with 6.5 cm diameter and 8 cm length containing spherical particles of carbon steel.

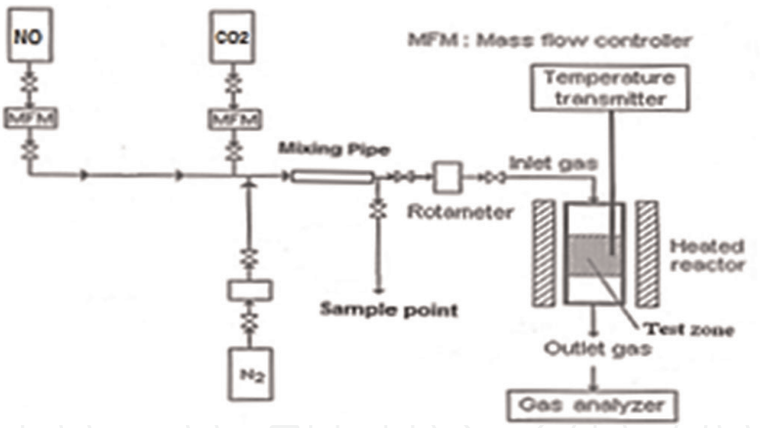

Figure 1.
Schematic of the experimental set-up.

N_2 and CO_2 were supplied by pressurized cylinders. The purity for CO_2, NO, and N_2 cylinders was 99.9, 99, and 99.99% (vol.%), respectively. The used concentrations of CO_2 were 10 and 13.725% (vol.%). Delivery of the feed gas was controlled by mass flow meter. After mixing in a mixing chamber (2.45 cm diameter and 15 cm length), simulated gas was fed into the inlet of the adsorber. Prior to all measurements, an initial degassing of the sample was performed at a given temperature (30, 50, 70, and 90°C) by the flow of nitrogen until reaching steady state. Then mixed gas was passed through the fixed bed column at constant temperature. The inlet and outlet concentrations were analyzed by a Testo 350XL flue gas, which has a resolution for N_2, NO, and CO_2 of 0.1 ppm, 0.1 ppm, and 0.1% vol., respectively. The total flow was kept constant for 12 l/min; whereas the N_2 and CO_2 were controlled precisely according to the required balance gas N2 during binary experiments. The dynamic adsorption capacity of CO_2 onto AC column was calculated using Eqs. (1) and (2) [10]:

$$t = \int_0^t \left(1 - \frac{c}{c_o}\right) dt \tag{1}$$

$$q_i = \frac{Q_v . y_i . t . \rho_i}{m} * 1000 \tag{2}$$

where t is the time of adsorption (min.), C is the outlet concentration of CO_2 gas (mg/l), C_o is the inlet concentration of CO_2 gas (mg/l), q_i is the amount of adsorbed gases (mg gas/g adsorbent), Q_v is the volumetric flow rate of CO_2 gas (l/min.), y_i is the mole fraction of inlet CO_2, ρ_i is the density of inlet gas (mg/l), and m is the weight of the adsorbent (g).

The interval times for measurements were 5, 10, 15, 20, 25, 30, 35, 40, 50, 60, 70, and 80 min. The experimental procedures and measurements are replicated three times for accuracy.

2.3 Adsorption isotherm studies

In order to optimize the design of a sorption system to capture CO_2 on AC, the suitable isotherm model for equilibrium curves must be established. Equilibrium models that have been examined herein are Langmuir, Freundlich, Temkin, and Dubinin-Radushkevich. The conformity between the predicted values of models and experimental data is expressed by comparing the experimental adsorption

capacity with the adsorption capacity estimated by these models, by means of the determination coefficient (r^2, values close or equal to 1) [11, 12].

2.3.1 The Langmuir isotherm

The widely used Langmuir isotherm found as a successful application in many real sorption processes [12] is expressed as

$$q_e = \frac{K_L C_e}{1 + a_L C_e} \tag{3}$$

A linear form of this expression is

$$\frac{C_e}{q_e} = \frac{1}{K_L} + \frac{a_L}{K_L} C_e \tag{4}$$

where q_e is the amount of adsorbed CO_2 per unit weight of AC at equilibrium (mg/g) and C_e is the unadsorbed CO_2 concentration in effluent at equilibrium (mg/l). K_L is the Langmuir equilibrium constant, and K_L/a_L value is used to estimate the theoretical monolayer capacity of AC, Q_o (mg/g). Therefore, the plot of C_e/q_e versus C_e enables one to determine the constants a_L and K_L.

2.3.2 The Freundlich isotherm

The well-known Freundlich isotherm is often used for heterogeneous surface energy systems [12]. The Freundlich equation is given as

$$q_e = K_F C_e^{1/n} \tag{5}$$

A linear form of this expression is

$$\log\, q_e = \log\, K_F + \frac{1}{n}\, \log\, C_e \tag{6}$$

where K_F is the Freundlich constant (mg/g) and n is the Freundlich exponent. K_F and n can be determined from the linear plot of $\log q_e$ versus $\log C_e$.

2.3.3 Temkin isotherm

The Temkin isotherm [13, 14] has been used in the following form:

$$q_e = \frac{RT}{b} \ln (A C_e) \tag{7}$$

A linear form of the Temkin isotherm can be expressed as

$$q_e = \frac{RT}{b} \ln A + \frac{RT}{b} \ln C_e \tag{8}$$

where A is the Temkin isotherm equilibrium binding constant (l/g), b is the Temkin isotherm constant, R is the universal gas constant (8.314 J/mol.K), T is the temperature, and B ($=RT/b$) is the constant related to heat of adsorption (J/mol).

The sorption data can be analyzed according to Eq. (8). Therefore, the plot of q_e versus $\ln(C_e)$ enables one to determine the constants A and B.

2.3.4 Dubinin-Radushkevich isotherm

The Dubinin-Radushkevich equation in Eq. (9) is as follows [15]:

$$q_e = q_m \, e^{-\beta\varepsilon^2} \tag{9}$$

A linear form of Dubinin-Radushkevich isotherm is

$$\ln q_e = \ln q_m - \beta\varepsilon^2 \tag{10}$$

where q_m is the Dubinin-Radushkevich monolayer capacity (mg/g), β is the Dubinin-Radushkevich isotherm constant (mol^2/kJ^2), and ε is the Polanyi potential, and it's related with equilibrium concentration as follows:

$$\varepsilon = \frac{RT}{M} \ln\left(1 + \frac{1}{C_e}\right) \tag{11}$$

where R is the universal constant of gases (8.314 J/mol.K), T is the experiment temperature (K), and M is the molecular weight of CO_2. The constant β gives the mean free energy of adsorption (E) for CO_2 molecules transported from the gas bulk to the surface of AC which is calculated by using Eq. (12) [14, 16]:

$$E = \frac{1}{\sqrt{2\beta}} \tag{12}$$

2.4 Kinetic models of adsorption

To determine an appropriate kinetic model is necessary to analyze the experimental data to investigate the mechanism of adsorption process that may include mass transfer or chemical reaction. Also, other extensive models applied to many models such as homogenous surface diffusion model and heterogeneous diffusion model (also known as pore and diffusion models, respectively) have been extensively applied to expound the adsorbate transfer onto the particles of adsorbent [17–19]. The determination coefficient (r^2) is used to examine the confirmation of the predicted values of models with experimental data (determination coefficient value close or equal to 1). The validity of these models is evaluated by the determination coefficient (r^2), which is within the range of 0–1, in which r^2 closer to unity implies the best fitting toward the particular kinetic model [20].

2.4.1 Simple first-order model

The sorption kinetic may be described by a simple order equation [21, 22]. The following simple first-order equation describes the change in bulk concentration:

$$C_t = C_o e^{k_1 t} \tag{13}$$

that can be rearranged to obtain a linear form

$$\log C_t = \frac{k_1}{2.303} t + \log C_o \tag{14}$$

where C_t and C_o are the concentration of adsorbate at time t and initially (mg/l), respectively, and k_1 is the first-order rate constant, (1/min).

Furthermore, Sparks [23] and Hossain et al. [21] proposed that the simple kinetic models such as first- or second-order rate equations are not applicable to the adsorption system with solid surfaces.

2.4.2 Pseudo-first-order model

The sorption kinetics may be described by pseudo-first Eq. (15) [13, 21, 24–26]:

$$\frac{dq_t}{dt} = k_1(q_e - q_t) \tag{15}$$

Integration of Eq. (15) and using the initial conditions $q_t = 0$ at $t = 0$ and $q_t = q_t$ at $t = t$ yield

$$\log\left(\frac{q_e}{q_e - q_t}\right) = \frac{k_1}{2.303}t \tag{16}$$

By rearrangement of Eq. (16), a linear form is obtained:

$$\log(q_e - q) = \log q_e - \frac{k_1}{2.303}t \tag{17}$$

where q_e is the amount of CO_2 adsorbed at equilibrium (mg/g), q is the amount of CO_2 adsorbed at time t (mg/g), and k_1 is the pseudo-first-order constant (1/min).

The pseudo-first-order constant k_1 and equilibrium adsorption q_e are determined by plot of $\log(q_e\text{-}q)$ versus t.

2.4.3 Pseudo-second-order model

The adsorption kinetics may also be described by pseudo-second-order Eq. (17) [13, 26–30]:

$$\frac{dq_t}{dt} = k_2(q_e - q_t)^2 \tag{18}$$

Integrating Eq. (18) and applying the initial boundaries yield

$$\frac{1}{(q_e - q_t)} = \frac{1}{q_e} + k_2 t \tag{19}$$

By rearrangement Eq. (19), a linear form is obtained:

$$\frac{t}{q_t} = \frac{1}{k_2 {q_e}^2} + \frac{1}{q_e}t \tag{20}$$

where k_2 is the equilibrium rate constant of pseudo-second-order adsorption (g/mg.min).

The slopes and intercepts of plots t/q_e versus t are used to calculate the pseudo-second-order rate constants k_2 and q_e.

2.4.4 Intra-particle diffusion model

The intra-particle diffusion model is expressed as [31–33]

$$q_t = k_p t^{0.5} + c \tag{21}$$

where k_p is a rate factor (present CO_2 adsorbed per minute). The plot of this model is multi-linear that indicates there are two or more steps occurring consecutively. The external surface/instantaneous adsorption stage occurred first in sharp portion. Then a gradual adsorption stage is in the second portion, where the controlled rate is the intra-particle diffusion. Final equilibrium stage occurs where intra-particle diffusion begins to slow down because of extremely low adsorbate concentrations in the bulk [24, 34].

2.5 Thermodynamic studies

Thermodynamic parameters were estimated from Langmuir isotherms by using the Van't Hoff's equation as in Eqs. (22) and (23). The thermodynamic parameters can be estimated from Langmuir isotherms by using the Van't Hoff's equation as follows [12, 35]:

$$\Delta G^o = -RTlna_L \tag{22}$$

$$\ln a_L = \frac{\Delta S^o}{R} - \frac{\Delta H^o}{RT} \tag{23}$$

where a_L is a Langmuir constant (l/mol), R is the universal constant of gases (8.314 J/mol.K), and T is an absolute temperature of gas.

3. Results and discussion

3.1 Adsorbent characterization

The main characteristics of AC (particle diameter, bed porosity, weight of bed, BET surface area, and pore volume) are shown in **Table 1**. Due to a high value BET surface area for used AC, its good pore structure makes it a suitable candidate for CO_2 capture.

3.2 Dynamic studies

Two mixtures of CO_2 and N_2 gases have been used in experiments (initial concentrations of CO_2 are 10 and 13.725% vol., respectively). **Figure 2** shows that

Characteristic	Value	Unit
Particle diameter	5	mm
Bed porosity	0.304	—
Weight of bed	500	g
BET surface area	602	m^2/g
Pore volume	0.61	cm^3/g

Table 1.
Characteristics of used AC depending on particle diameter.

the rate of CO_2 adsorption gradually decreased with time, until equilibrium condition was achieved. This behavior is observed for each line in **Figures 2** and **3** throughout a gradual increase of the concentration ratio of (outlet/initial) concentrations of CO_2 (C/C_o).

The CO_2 adsorption was most intensive during 50 min. and thereafter remains unchanged until saturation was attained. Adsorption process to carbon dioxide for different temperatures (30, 50, 70, and 90°C) on AC reaches equilibrium for increased temperature. The same behavior is shown in **Figure 3** when using a high concentration of carbon dioxide but fast (30 min. to reach the equilibrium), due to high CO_2 concentration, and this behavior is compatible with previous results when using AC prepared from coconut residue to remove carbon dioxide [36]. It is noted that breakthrough curves become shorter and steeper for high temperatures; this indicates the adsorption process here is exothermic and that's compatible with previous results for some of the previous adsorption of carbon dioxide on the zeolite [1]. The adsorption of carbon dioxide carbon process was not affected by the presence of nitrogen gas, and this is due to the strength of the links formed by carbon dioxide with AC particles [36].

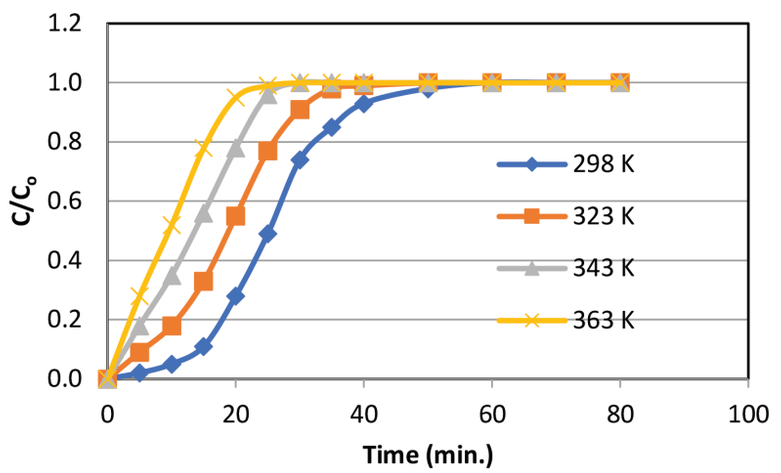

Figure 2.
Breakthrough curve for CO_2 adsorption onto AC (initial conc. = 10%vol., avg. particle diameter = 5 mm, and volumetric rate = 12 l/min).

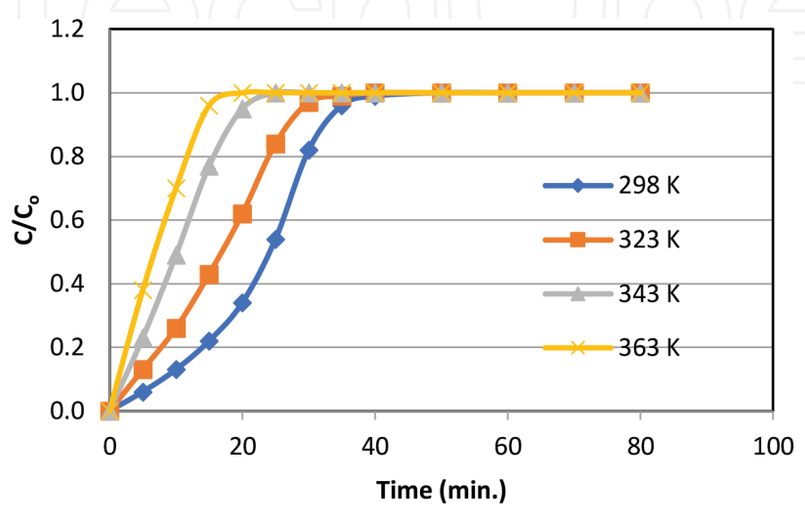

Figure 3.
Breakthrough curve for CO_2 adsorption onto AC (initial conc. = 13.725%vol., avg. particle diameter = 5 mm, and volumetric rate = 12 l/min).

In post-combustion process, the flue gas temperature is typically within the range of 50–120°C [36, 37]. Thus, an adsorption study was conducted at 30–90°C to investigate the CO_2 adsorptive properties at elevated temperatures. **Figures 4** and **5** show that the CO_2 adsorption capacity of solid adsorbent decreases with temperature, and it implies the existence of physical adsorption (physisorption) between the CO_2 molecules and carbonaceous adsorbent. Adsorption capacity decreased with increasing temperature because of exothermic adsorption process as shown in **Figures 4** and **5**. This behavior is also identical with the results of previous studies [3, 38]. The adsorption capacities recorded in **Figure 4** are 109.529, 74.57, 50.61, and 35.46 $mg_{(CO2)}/g_{AC}$, whereas they recorded in **Figure 5** as 129.651, 89.2, 53.079, and 35.546 $mg_{(CO2)}/g_{AC}$ at temperatures 30, 50, 70, and 90°C, respectively. Thus, the optimum temperature for the removal process is 30°C. It also notices that the adsorption process occurs in the beginning quickly and be a decline in the curves and clear because of the abundance of the active sites and the presence of small surface resistance on the surface of adsorbents, then more smoothness gradually less steep and alignment over time because of the fullness of all the active sites on the surface of adsorbents and that the process has become controlled by internal diffusion within the adsorbents in accordance with what has been presented previously [39]. Also the results of comparison for both **Figures 4** and **5** together note

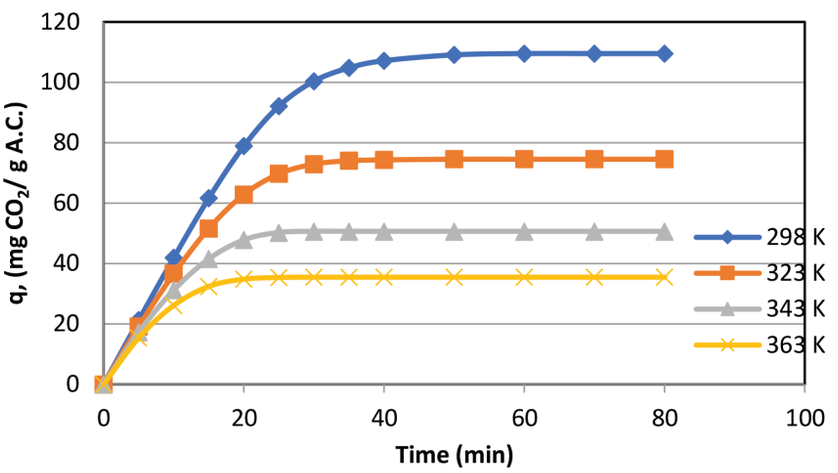

Figure 4.
Adsorption capacity of CO_2 onto AC (initial concn. = 10%vol., avg. particle diameter = 5 mm, and volumetric rate = 12 l/min.).

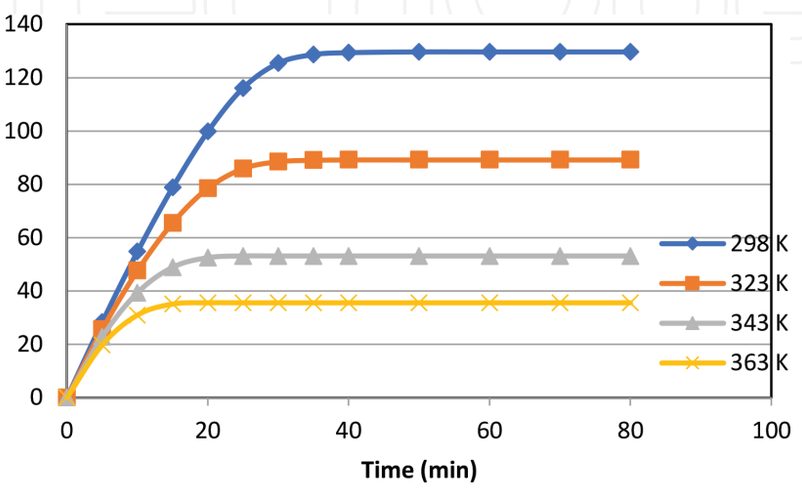

Figure 5.
Adsorption capacity of CO_2 onto AC (initial conc. = 13.725%vol., avg. particle diameter = 5 mm, and volumetric rate = 12 l/min.).

that the amount of the CO_2 adsorbed onto AC increases due to increase of the concentration difference of CO_2 between bulk and surface of AC leading to an increase of mass transfer [9, 40].

3.3 Equilibrium isotherm studies

The equilibrium data can be approximated using common and practical adsorption isotherms, which provide the basis for the design of adsorption systems. The amount of adsorbed CO_2 onto adsorbent (AC) as a function of its concentration at constant temperature can be described by different adsorption isotherm models (Langmuir, Freundlich, Temkin, and Dubinin-Radushkevich). The predicted isotherm constants for the CO_2 adsorption and the determination coefficient r^2 value from the linear regression method are shown in **Table 2**.

Based on tabulated data, the maximum capacity (Q_o) of AC and a_L values (Langmuir parameters) for CO_2 adsorption decreased with increasing temperature; this reveals a physisorption process occurred. The decline in values of maximum adsorption capacity with increased in the adsorption temperature is due to the exothermic nature of the CO_2 adsorption on AC. It is confirmed by n values higher than 1 in the Freundlich isotherm model that the adsorption is favorable for AC.

C_o	T	*Langmuir constants*		*Freundlich constants*		Q_{exp}	Q_L	r^2	Q_F	r^2
Vol. %	**°C**	**a_L (l/mg)**	**Q_o (mg/g)**	**K_F (mg/g)**	**n (−)**	**(mg/g)**	**(mg/g)**	**—**	**(mg/g)**	**—**
10	30	0.0492	120.482	0.00081	0.3865	109.53	108.03	0.997	522.49	0.955
	50	0.01835	99.009	0.04223	0.527	74.57	90.633	0.9976	685.26	0.954
	70	0.01076	81.301	0.2138	0.5998	50.61	50.92	0.9865	966.67	0.964
	90	0.00778	66.667	0.5181	0.6342	35.46	49.835	0.9829	1358.19	0.972
13.725	30	0.01171	161.29	0.002202	0.5324	129.65	129.693	0.9976	649.62	0.936
	50	0.0921	133.333	0.0933	0.5821	89.2	89.92	0.9919	1024.09	0.959
	70	0.0782	85.47	0.1711	0.5596	53.08	53.2934	0.9964	2453.47	0.982
	90	0.0466	67.11	0.6192	0.5996	35.55	35.78	0.9872	6014.59	0.984
C_o	**T**	**Temkin constants**		**D-R constants**		**Q_{exp}**	**Q_T**	**r^2**	**Q_{D-R}**	**r^2**
Vol. %	**°C**	**B (J/mol)**	**A (l/g)**	**ß (mol^2/kJ^2)**	**q_m (mg/g)**	**ε (kJ/mol)**	**(mg/g)**	**(mg/g)**	**—**	**(mg/g)**	**—**
10	30	22.305	0.746	0.0078	93.841	8.006	109.53	108.84	0.998	93.76	0.806
	50	22.582	0.167	0.0881	70.316	2.382	74.57	75.009	0.997	69.48	0.909
	70	19.114	0.092	0.221	51.07	1.506	50.61	50.965	0.994	49.16	0.955
	90	15.473	0.067	0.339	37.68	1.123	35.46	35.58	0.996	35.02	0.982
13.725	30	35.826	0.164	0.104	117.47	2193	129.65	131.45	0.989	116.78	0.86
	50	30.949	0.0813	0.308	86.59	1.27	89.2	89.93	0.996	84.62	0.923
	70	20.395	0.0642	0.519	54.806	0.981	53.08	53.24	0.998	52.21	0.968
	90	16.048	0.0378	1.276	39.186	0.626	35.55	35.63	0.9947	35.43	0.996

Table 2.
Parameters of isotherm models at different temperatures via linearized technique for adsorption of CO_2 onto AC.

In addition, the Dubinin-Radushkevich isotherm will provide a useful information related to the energy parameters, in terms of E (mean free energy of adsorption). The calculated E values which are within the range of 1.213–8 and 0.626–2.193 kJ/mol for both initial concentrations 10 and 13.725% vol., respectively, suggest that the CO_2 adsorption is physical in nature, as the magnitude of E is below 8 kJ/mol, whereas the value of $8 < E < 16$ is an indicator of the chemical adsorption [41]. Also, B (value of heat adsorption) in Temkin isotherm ranged between 15.47 and 35.826 J/mol indicating a physisorption process occurs.

On the basis of corresponding r^2 values and adsorption capacity estimated by each model shown in **Table 2**, the Langmuir model gives the best fit toward the experimental data over the entire temperature range. Therefore, it implies that the surface of the activated carbon is heterogeneous and a restricted monolayer CO_2 adsorption occurs, as results of adsorption CO_2 onto activated carbon prepared from coconut fiber studied by Hauchhum and Mahanta [3].

3.4 Kinetic studies

An analysis of kinetic adsorption process is a useful tool to estimate the time of residence for the adsorption process to complete and to determine the dynamics of adsorption and its performance in industrial scale of fixed bed or in flow-through systems. Thus, simple first-order, pseudo-first-order, pseudo-second-order, and intra-particle diffusion models were performed in this study. Kinetic parameters of these models are shown in **Table 3**.

Table 3 shows the simple first-order kinetic model for activated carbon did not fit well with the experimental data, with r^2 value found to be within the range of 0.4344–0.7873 and 0.319–0.734 for both initial concentrations 10 and 13.725% vol., respectively. Also, **Table 3** shows the pseudo-first-order kinetic model for activated carbon did not fit well with the experimental data, with r^2 value found to be within the range of 0.9521–0.967 also from 0.9175 to 0.9487 for both initial concentrations 10 and 13.725% vol., respectively.

Comparing the values of determination coefficients as stated in **Table 3**, pseudo-second-order model gives better fit than the pseudo-first-order and intra-particle diffusion models with experimental data, with r^2 value within the range of 0.963–0.996 and 0.955–0.998 for both initial concentrations 10 and 13.725% vol., respectively. Also, the values of adsorption capacity of equilibrium (q_e) were observed to decrease with respect to temperature. The kinetic energy of CO_2 adsorbed at elevated temperatures is high, and it leads to its increasing tendency to escape from the AC surface. Maroto-Valer et al. [42] reported that physisorption process involves high surface adsorption energy and molecule diffusion at elevated temperatures, which result in instability of the adsorbed gas on the surface of activated carbon, and consequently desorption process will occur.

In similarity to pseudo-first-order and pseudo-second-order models, the intra-particle diffusion model provides insight of the mechanism in adsorption process. Adsorption contains of few steps involved in the transfer of adsorbate (CO_2) from the phase of bulk to the solid surface of AC and is followed by the molecule diffusion into the interior of the pores of AC. Intra-particle diffusion is typically described as a slow process and is a limiting step in many adsorption processes. Theoretically, if the adsorption process obeys the intra-particle diffusion model, a straight linear plot that passes through the origin is expected. However, results of the variation of gradient with respect to time show that the intra-particle diffusion is not the sole rate-limiting step in this adsorption process. Note that the first

Kinetic model	C_o (vol.%)	Parameter	Temperature (°C)			
			30	50	70	90
Simple first-order	10	k_1	2.633	1.974	1.394	0.955
		C_o	4.1×10^5	1.75×10^{21}	1.67×10^{33}	6.73×10^{40}
		r^2	0.787	0.667	0.539	0.434
	13.725	k_1	3.293	2.404	1.457	1.091
		C_o	3.04×10^{17}	8.414×10^{36}	6.52×10^{56}	1.023×10^{80}
		r^2	0.734	0.624	0.427	0.319
Pseudo-first-order	10	k_1	0.0972	0.1521	0.1864	0.2367
		q_e	159.48	143.481	84.94	62.22
		r^2	0.967	0.96	0.915	0.952
	13.725	k_1	0.1508	0.182	0.2116	0.282
		q_e	292.89	195.45	78.25	49.47
		r^2	0.918	0.927	0.944	0.949
Pseudo-second-order	10	k_2	1.6×10^5	6.59×10^4	3.14×10^4	1.69×10^4
		q_e	144.93	87.719	55.56	37.45
		r^2	0.968	0.976	0.989	0.995
	13.725	k_2	2.88×10^5	1.29×10^5	5.76×10^4	3.23×10^4
		q_e	161.29	102.04	56.179	36.496
		r^2	0.96	0.982	0.955	0.998
Intra-particle diffusion	10	k_p	13.974	8.755	5.436	3.489
		c	7.686	12.25	13.025	11.775
		r^2	0.874	0.8123	0.7417	0.6811
	13.725	k_p	15.976	10.169	5.219	3.151
		c	14.137	17.633	17.693	14.578
		r^2	0.841	0.788	0.677	0.601

Table 3.
Kinetic parameters of CO_2 onto AC.

steeper region (2–4 $min.^{1/2}$) could be due to surface sorption, while the second region (4–9 $min.^{1/2}$) may be attributed by the intra-particle diffusion rate controlled.

3.5 Thermodynamic studies

The values of thermodynamic parameters of CO_2 adsorption process on AC based on Van't Hoff plot for Eqs. (22) and (23) are shown in **Figure 6**.

The estimated values of the thermodynamic parameters are tabulated in **Table 4**. For significant adsorption to occur, the Gibbs free energy change of adsorption (ΔG^o) must be negative [43]. **Table 4** shows that the (ΔG^o) was negative values for all five temperatures studied, which indicates the feasibility and spontaneity of the adsorption process. In addition, decreased negative ΔG^o value with increasing temperature implies that the CO_2 adsorption process is more favorable at 30°C rather than at 90°C; this behavior is also noticed by Rashidi et al. [44] and Hauchhum and Mahanta [3].

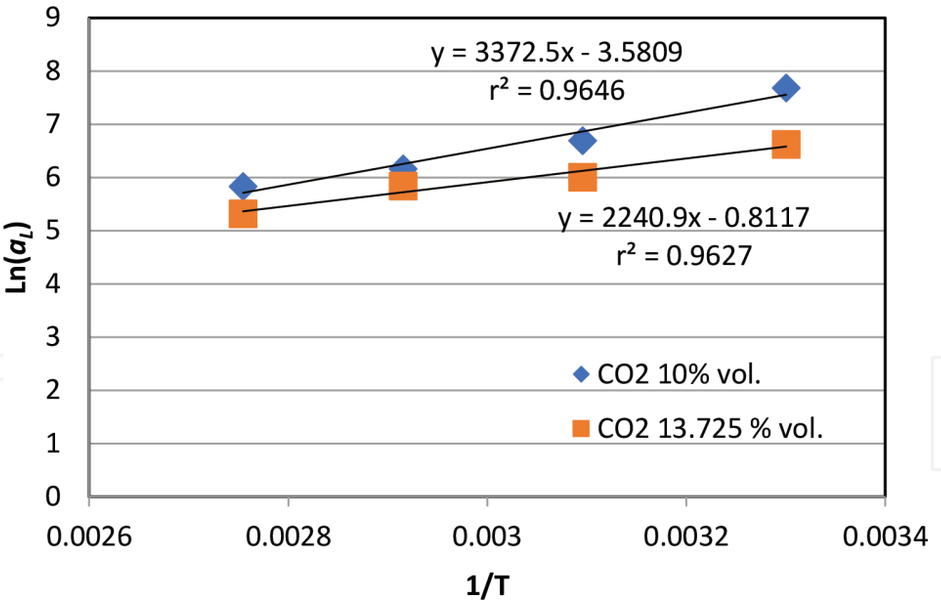

Figure 6.
Van't Hoff plot for adsorption of CO_2/AC system.

Conc.	Temp.	a_L	ΔG^o	ΔH^o	ΔS^o
(vol.%)	(K)	(mol/l)	(J/mol)	(J/mol)	(J/mol.K)
10	303	2164.79	−19347.21	−28038.965	−29.7716
	323	807.71	−17976.75		
	343	473.45	−17566.61		
	363	342.50	−17613.77		
13.725	303	753.38	−16688.24	−18630.843	−6.748
	323	405.31	−16124.99		
	343	344.14	−16065.94		
	363	204.91	−16063.38		

Table 4.
Thermodynamic parameters of CO_2 adsorption onto AC.

According to findings of the experimental data, the negative sign of ΔH^o value indicates an exothermic nature of the CO_2 adsorption process onto AC, and the negative value of ΔS^o suggests high orderliness of the adsorbate molecules (CO_2) upon adsorption. Zhao et al. [45] mentioned that the negative value of ΔS^o can be interpreted by the behavior of the CO_2 molecules upon the adsorption process, which is from randomized to an ordered form on the surface of the adsorbent. The decline in the entropy value upon the adsorption process is due to a lesser degree of freedom of the CO_2 molecules, due to minimum free space on the surface of AC. Moreover, the value of ΔH^o indicates the type of CO_2 adsorption process, whether it belongs to the physisorption or chemisorption. It has been reported that the value of ΔH^o for the physisorption process is <20 kJ/mol, while for the chemisorption process, the value is within 80–200 kJ/mol [45, 46]. Therefore, the calculated values of ΔH^o approximately ranging between 18 and 28 kJ/mol suggest that the CO_2 adsorption can be attributed to a physi-intra-particle diffusion adsorption process rather than a pure physisorption or chemisorption process. Also, this supports the isotherm study results that reveal the adsorption mechanism is physisorption and obeys Langmuir isotherm model.

3.6 Effects of interaction between gases in mixture

The adsorption amount for each component in a complex mixture of (CO_2, NO, and N_2) was compared with that under the single-component conditions, with the results shown in **Figure 7**. In the single-component condition, the adsorption amount was 109.24 mg_{CO2}/g_{AC} and 0.245 mg_{NO}/g_{AC} in 50 and 40 min for each one, respectively. When all of the components were present in a mixture of CO_2, NO, and N_2, the CO_2 adsorption amount decreased by 6%, and the NO adsorption amount also decreased by 7.6%. The adsorption capacity of CO_2 in complex mixture is not changed compared with that under the single-component conditions but is favorable due to decreased equilibrium time required. The adsorption capacities of complex mixture were 103.2 mg_{CO2}/g_{AC} in 40 min and 0.229 mg_{NO}/g_{AC} in 30 min. This decrease in adsorption capacity is due to the competition between both gases on the active sites, whereas the CO_2 adsorption capacity is higher than NO gas because of the presence of CO_2 gas at high concentrations. NO and CO_2 display fast breakthrough, and high adsorption amounts were observed in the pure component adsorption experiments. When the interaction effect of CO_2 and NO was considered, a very interesting phenomenon appeared. After the initial breakthrough, the CO_2 concentration descends to a minimum and then gradually ascends with the breakthrough ending point of NO. This is observed from the arrival time of the

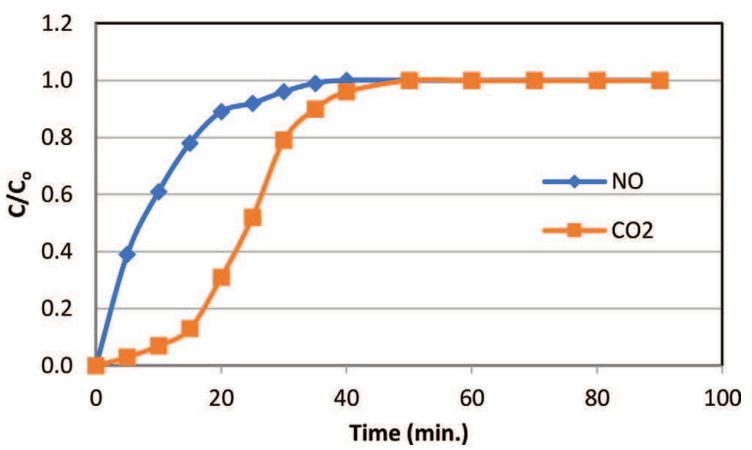

Figure 7.
Breakthrough curves for mixture gas (CO_2, NO, and N_2) (initial conc. = 10% vol. of CO_2, and 550 ppm of NO, avg. particle diameter = 5 mm, temperature = 30°C, and volumetric rate = 12 l/min.)

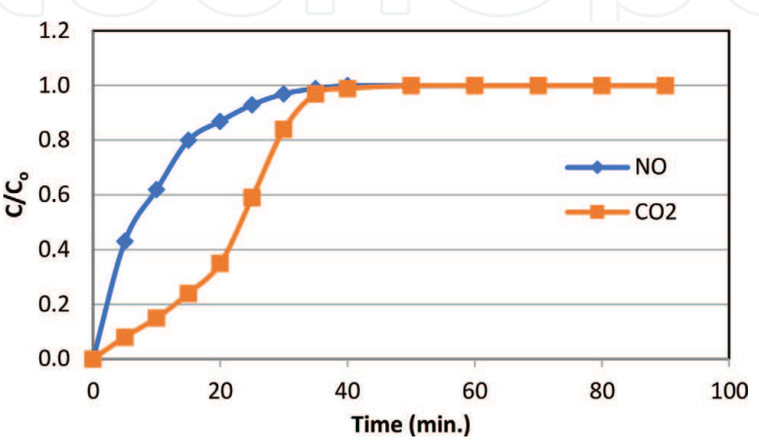

Figure 8.
Breakthrough curves for mixture gas (CO_2, NO, and N_2) (initial conc. = 13.725%vol. of CO_2, and 550 ppm of NO, avg. particle diameter = 5 mm, temperature = 30°C, and volumetric rate = 12 l/min.)

equilibrium state which was 30 min for the NO gas and 40 min for the CO_2 gas; the same behavior is shown for the single-component conditions; the difference between them was reached in the equilibrium stage fast approximately 10 min. In **Figure 8** the adsorption capacities of complex mixture were 124.4 mg_{CO2}/g_{AC} in 40 min and 0.22 mg_{NO}/g_{AC} in 30 min by using different initial concentrations of gases. This is confirmed by the fact that free Gibbs energy values of both gases are very different, as they have NO gas higher in value, while in the case of CO_2, they are much lower. This behavior is shown in previous study for adsorption on activated carbon prepared from coconut husk residues [47].

4. Conclusion

In this study, the fixed bed adsorption of carbon dioxide from CO_2/N_2 mixtures on activated carbon was studied. The adsorption dynamics was investigated at different operating temperatures (30–90°C). The results show that the low-cost activated carbon can be prepared from olive trees as potential carbonaceous material serving as porous media for CO_2 capture. Based on the experimental results, it is concluded that the CO_2 adsorption onto the olive tree activated carbon follows the physisorption behavior, whereby the CO_2 adsorption capacity decreases with respect to increasing temperature. Based on the equilibrium models of isotherm used herein to fit the experimental data of adsorption, the Langmuir model was the best fit with experimental data over the whole temperature range, due to the highest estimated adsorption capacity and determination coefficient (r^2) closeness to unity, thus implying a perfect fit to the experimental data. Besides, thermodynamic analysis proves that the CO_2 adsorption is a spontaneous process at low temperature, physisorption, and intra-particle diffusion and exothermic in nature. Also, the negative values of the entropy of the adsorption manifest the restricted randomness of the adsorbate molecules on the surfaces of adsorbent. CO_2 adsorption capacity has been reduced slightly when NO appears, but the process of adsorption has been faster as a result of competition on carbon-active sites.

Olive trees are dominant and easily available in the Mediterranean countries generally and especially Libya, and because charcoal is prepared from olive trees, it is cheap in Libya. According to the obtained result, this study concludes that AC prepared from olive trees can be considered as adequate for designing a fixed bed cycle to separate carbon dioxide from flue gases and serve as a benchmark while searching for inexpensive and superior activated carbon production in future studies that concerned of capturing CO_2 from flue gases of the industrial sectors (such as cement plants and power stations) that are prevailing in Libya.

Author details

Hesham G. Ibrahim[1*] and Mohamed A. Al-Meshragi[2]

1 Mechanical Engineering Department, Faculty of Marine Resources, Al-Asmarya Islamic University, Zliten, Libya

2 Chemical Engineering Department, University of Tripoli, Tripoli, Libya

*Address all correspondence to: h.ibrahim@asmarya.edu.ly

IntechOpen

References

[1] Dantas TLP, Luna FMT, Silva Jr IJ, Torres AEB, de Azevedo DCS, Rodrigues AE, et al. Modeling of the fixed-bed adsorption of carbon dioxide and a carbon dioxide-nitrogen mixture on zeolite 13x. Brazilian Journal of Chemical Engineering. 2011;**28**(3): 533-544. DOI: 10.1590/S0104-66322011000300018

[2] Zhao Z, Cui X, Ma J, Li R. Adsorption of carbon dioxide on alkaline-modified zeolite 13X adsorbents. The International Journal of Greenhouse Gas Control. 2007;**1**(3):355-357. DOI: 10.1016/s1750-5836(07)00072-2

[3] Hauchhum L, Mahanta P. Kinetic, thermodynamic and regeneration studies for CO_2 adsorption onto activated carbon. International Journal of Advanced Mechanical Engineering. 2004;**4**(1):27-32. Available from: https://pdfs.semanticscholar.org/eacc/3f82336a3276744eda9a898c4621da7d357d.pdf

[4] Grande CA, Rodrigous AE. Electric swing adsorption for CO_2 removal from flue gases. International Journal of Greenhouse Gas Control. 2008;**2**: 194-202. DOI: 10.1016/s1750-5836(07)00116-8

[5] Cavenati S, Grande CA, Rodrigues AE. Separation $CH_4/CO_2/N_2$ mixtures by layered pressure swing adsorption for upgrade of natural gases. Chemical Engineering Science. 2006;**61**: 3893-3906. DOI: 10.1016/j.ces.2006.01.023

[6] Chen LC, Peng PY, Lin LF, Yang TCK, Huang CM. Facile preparation of nitrogen-doped activated carbon for carbon dioxide adsorption. Aerosol and Air Quality Research. 2014;**14**:916-927. DOI: 10.4209/aaqr.2013.03. 0089

[7] Zeinali F, Ghoreyshi AA, Najafpour GD. Adsorption of dichloromethane from aqueous phase using granular activated carbon: Isotherm and breakthrough curve measurements. Middle-East Journal of Scientific Research. 2010;**5**(4):191-198. DOI: 10.1080/00986445.2011.584354

[8] Alshuiref AA, Ibrahim HG, Ben Mahmoud MM, Maraie AA. Treatment of wastewater contaminated with Cu(II) by adsorption onto acacia activated carbon. Journal of Marine Sciences and Environmental Technologies (JMSET). 2017;**3**(2):25-36 Available from: http://www.asmarya.edu.ly/journal2/wp-content/uploads/2018/04/JMSET03-3-2-2017.pdf

[9] Kuboňová L, Obalová L, Vlach O, Troppová I, Kalousek J. Modeling of NO adsorption in fixed bed on activated carbon. Chemical and Process Engineering. 2011;**32**(4):367-377. DOI: 10.2478/v10176-011-0029-z

[10] McCabe W, Smith J, Harriott P. Unit Operations of Chemical Engineering. 7th ed. NY, USA: McGraw Hill Chemical Engineering Series; 2004. ISBN-10: 0072848235

[11] Khalili S, Ghoreyshi A, Jahanshai M. Carbon dioxide captured by multi-walled carbon nanotube and activated charcoal: A comparative study. Chemical Industry & Chemical Engineering. 2013;**19**(1):153-164. DOI: 10.2298/ciceq120217050k

[12] Ibrahim HG. Removal and Recovery of Chromium from Aqueous Solutions. Saarbrucken, Germany: LAP Lambert Academic Publishing GmbH and Co. KG; 2010; ISBN-10: 3838339037

[13] Özacar M. Adsorption of phosphate from aqueous solution onto alunite. Chemosphere. 2003;**51**(4):321-327. DOI: 10.1016/s0045-6535(02)00847-0

[14] Choy KK, McKay G, Porter JF. Sorption of acid dyes from effluents using activated carbon. Resources,

Conservation and Recycling. 1999;**27**(1–2):57-71. DOI: 10.1016/s0921-3449(98)00085-8

[15] Carrasco-Marin F, Lopez-Ramon MV, Moreno-Castilla C. Applicability of the Dubinin-Radushkevich equation to carbon dioxide adsorption on activated carbons. Langmuir. 1993;**9**(11):2758-2760. DOI: 10.1021/-la00035a002

[16] Lin SH, Juang RS. Heavy metal removal from water by sorption using surfactant-modified montmorillonite. Journal of Hazardous Materials. 2002;**92**(3):315-326. DOI: 10.1016/s0304-3894(02)00026-2

[17] Fadali OA, Magdy YH, Daifullah AAM, Ebrahiem EE, Nassar MM. Removal of chromium from tannery effluents by adsorption. Journal of Environmental Science and Health. 2004;**39**(2):465-472. DOI: 10.1081/ese-120027537

[18] Yang H, Xu Z, Fan M, Gupta R, Slimane RB, Bland AE, et al. Progress in carbon dioxide separation and capture: A review. Journal of Environmental Sciences. 2008;**20**:14-27. DOI: 10.1016/S1001-0742(08)60002-9

[19] Raven KP, Jain A, Loeppert RH. Arsenite and arsenate adsorption on ferrihydrite: Kinetics, equilibrium, and adsorption envelopes. Environmental Science & Technology. 1998;**32**(3):344-349. DOI: 10.1021/es970421p

[20] Al-Meshragi M, Ibrahim HG, Okasha AY. Removal of trivalent chromium from aquatic environment by cement kiln dust: Batch studies. AIP Conf. Proc. 2009;**1127**(1):74-85. DOI: 10.1063/1. 3146200

[21] Hossain MA, Kumita M, Michigami Y, Mori S. Optimization of parameters for Cr (VI) adsorption on used black tea leaves. Adsorption. 2005;**11**(5–6):561-568. DOI: 10.1007/s10450-005-5613-4

[22] Eligwe CA, Okolue NB. Adsorption of iron (II) by a Nigerian brown coal. Fuel. 1994;**73**(4):569-572. DOI: 10.1016/0016-2361(94)90042-6

[23] Sparks DL. Kinetics of Soil Chemical Processes. 1st ed. Massachusetts, USA: Academic Press; 1989. DOI: 10.1016/b978-012656446-4/50007-4

[24] Annadurai G, Juang RS, Lee DJ. Use of cellulose-based wastes for adsorption of dyes from aqueous solutions. Journal of Hazardous Materials. 2002;**92**(3):263-274. DOI: 10.1016/s0304-3894(02)00017-1

[25] Özacar M, Şengil IA. Adsorption of reactive dyes on calcined alunite from aqueous solutions. Journal of Hazardous Materials. 2003;**98**(1–3):211-224. DOI: 10.1016/s0304-3894(02)00358-8

[26] Ho YS, Chiang CC. Sorption studies of acid dye by mixed sorbents. Adsorption. 2001;**7**(2):139-147. DOI: 10.1023/A:1011652224816

[27] Chiou MS, Li HY. Equilibrium and kinetic modeling of adsorption of reactive dye on cross-linked chitosan beads. Journal of Hazardous Materials. 2002;**93**(2):233-248. DOI: 10.1016/s0304-3894(02)00030-4

[28] Wu FC, Tseng RL, Juang RS. Kinetic modeling of liquid-phase adsorption of reactive dyes and metal ions on chitosan. Water Research. 2001;**35**(3):613-618. DOI: 10.1016/s0043-1354(00)00307-9

[29] Wu FC, Tseng RL, Juang RS. Kinetics of color removal by adsorption from water using activated clay. Environmental Technology. 2001;**22**(6):721-729. DOI: 10.1080/09593332208618235

[30] Ho YS, McKay G. Pseudo-second order model for sorption processes.

Process Biochemistry. 1999;**34**(5): 451-465. DOI: 10.1016/s0032-9592(98)00112-5

[31] Srivastava SK, Tyagi R, Pant N. Adsorption of heavy metal ions on carbonaceous material developed from the waste slurry generated in local fertilizer plants. Water Research. 1980; **23**(9):1161-1165. DOI: 10.1016/0043-1354(89)90160-7

[32] Shiue A, Hu SC, Chang SM, Ko TY, Hsieh A, Chan A. Adsorption kinetics and breakthrough of carbon dioxide for the chemical modified activated carbon filter used in the building. Sustainability. 2017;**9**(9):1-13. DOI: 10.3390/su9091533

[33] Demirbaş E, Kobya M, Öncel S, Şencan S. Removal of Ni(II) from aqueous solution by adsorption onto hazelnut shell activated carbon: Equilibrium studies. Bioresource Technology. 2002;**84**(3):291-293. DOI: 10.1016/s0960-8524(02)00052-4

[34] Sahmoune MN, Louhab K, Boukhiar A, Addad J, Barr S. Kinetic and equilibrium models for the biosorption of Cr(III) on Streptomyces rimosus. Toxicological and Environmental Chemistry. 2009;**91**(7):1291-1303. DOI: 10.1080/02772240802613731

[35] Wang S, Li H. Dye adsorption on unburned carbon: Kinetics and equilibrium. Journal of Hazardous Materials. 2005;**126**(1–3):71-77. DOI: 10.1016/j.jhazmat.2005.05.049

[36] Rashidi NA, Yusup S, Loong LH. Kinetic studies on carbon dioxide capture using activated carbon. Chemical Engineering Transaction, AIDIC Publications. 2013;**35**:361-366. DOI: 10.3303/CET1335060

[37] Kaithwas A, Prasad M, Kulshreshtha A, Verma S. Industrial wastes derived solid adsorbents for CO_2 capture: A mini review. Chemical Engineering Research and Design. 2012;**90**:1632-1641. DOI: 10.1016/j.cherd.2012.02.011

[38] Guo B, Chang L, Xiel K. Adsorption of carbon dioxide on activated carbon. Journal of Natural Gas Chemistry. 2006; **15**(3):223-229. DOI: 10.1016/S1003-9953(06)60030-3

[39] Li A, Wu H, Zhang Q, Zhang G, Long C, Fei Z, et al. Thermodynamic study of adsorption of phenolic compounds from aqueous solution by a water-compatible hypercrosslinked polymeric adsorbent. Chinese Journal of Polymer Science. 2004;**22**(3):259-267

[40] Thomas WJ, Crittenden B. The Literature of Adsorption. Adsorption Technology and Design. Massachusetts, USA: Butterworth-Heinemann; 1989. DOI: 10.1016/b978-075061959-2/50009-4

[41] Soltani DC, Safari M, Rezaee A, Godini H. Application of a compound containing silica for removing ammonium in aqueous media. Environmental Progress & Sustainable Energy. 2014;**34**(1):105-111. DOI: 10.1002/ep.11969

[42] Maroto-Valer MM, Tang Z, Zhang Y. CO_2 capture by activated and impregnated anthracites. Fuel Processing Technology. 2005;**86**: 1487-1502. DOI: 10.1016/j.fuproc.2005.01.003

[43] Saha P, Chowdhury S. Insight into adsorption thermodynamics. In: Tadashi M, editor. Thermodynamics. Rijeka: InTech; 2011. DOI: 10.5772/13474

[44] Rashidi NA, Yusup S, Borhan A. Isotherm and thermodynamic analysis of carbon dioxide on activated carbon. Procedia Engineering. 2016;**148**: 630-637. DOI: 10.1016/j.proeng.2016.06.527

[45] Zhao Y, Wang D, Xie H, Won SW, Cui L, Wu G. Adsorption of Ag (I) from aqueous solution by waste yeast: Kinetic, equilibrium and mechanism studies. Bioprocess and Biosystems Engineering. 2015;**38**(1):69-77. DOI: 10.1007/s00449-014-1244-z

[46] Liang S, Guo X, Feng N, Tian Q. Isotherms, kinetics and thermodynamic studies of adsorption of Cu^{2+} from aqueous solutions by Mg^{2+}/K^{+} type orange peel adsorbents. Journal of Hazardous Materials. 2010;**174**(1–3): 756-762. DOI: 10.1016/j.jhazmat.2009.09.116

[47] Yi H, Wang Z, Liu H, Tang X, Ma D, Zhao S, et al. Adsorption of SO_2, NO, and CO_2 on activated carbons: Equilibrium and thermodynamics. Journal of Chemical & Engineering Data. 2014;**59**(5):1556-1563. DOI: 10.1021/je4011135